Inorganic Chemistry

Article

pubs.acs.org/IC

New Monodentate Amidine Superbasic Ligands with a Single Configuration in *fac*-[Re(CO)$_3$(5,5′- or 6,6′-Me$_2$bipyridine)(amidine)]BF$_4$ Complexes

Pramuditha Abhayawardhana, Patricia A. Marzilli, Theshini Perera, Frank R. Fronczek, and Luigi G. Marzilli*

Department of Chemistry, Louisiana State University, Baton Rouge, Louisiana 70803, United States

Supporting Information

ABSTRACT: Treatment of two precursors, *fac*-[Re(CO)$_3$(L)(CH$_3$CN)]BF$_4$ [L = 5,5′-dimethyl-2,2′-bipyridine (5,5′-Me$_2$bipy) (**1**) and 6,6′-dimethyl-2,2′-bipyridine (6,6′-Me$_2$bipy) (**2**)], with five C_2-symmetrical saturated heterocyclic amines yielded 10 new amidine complexes, *fac*-[Re(CO)$_3$(L)(HNC(CH$_3$)N(CH$_2$CH$_2$)$_2$Y)]BF$_4$ [Y = CH$_2$, (CH$_2$)$_2$, (CH$_2$)$_3$, NH, or O]. All 10 complexes possess the novel feature of having only one isomer (amidine *E* configuration), as established by crystallographic and ^{1}H NMR spectroscopic methods. We are confident that NMR signals of the other possible isomer (amidine *Z* configuration) would have been detected, if it were present. Isomers are readily detected in closely related amidine complexes because the double-bond character of the amidine C−N3 bond (N3 is bound to Re) leads to slow *E* to *Z* isomer interchange. The new *fac*-[Re(CO)$_3$(L)(HNC(CH$_3$)N(CH$_2$CH$_2$)$_2$Y)]BF$_4$ complexes have C−N3 bonds with essentially identical double-bond character. However, the reason that the *Z* isomer is so unstable as to be undetectable in the new complexes is undoubtedly because of unfavorable clashes between the equatorial ligands and the bulky N(CH$_2$CH$_2$)$_2$Y ring moiety of the axial amidine ligand. The amidine formation reactions in acetonitrile (25 °C) proceeded more easily with **2** than with **1**, indicating that the distortion in 6,6′-Me$_2$bipy resulting from the proximity of the methyl substituents to the inner coordination sphere enhanced the reactivity of the coordinated CH$_3$CN. Reaction times for **1** and **2** exhibited a similar dependence on the basicity and ring size of the heterocyclic amine reactants. Moreover, when the product of the reaction of **1** with piperidine, *fac*-[Re(CO)$_3$(5,5′-Me$_2$bipy)(HNC(CH$_3$)N(CH$_2$CH$_2$)$_2$CH$_2$)]BF$_4$, was challenged in acetonitrile-d_3 or CDCl$_3$ with a 5-fold excess of the strong 4-dimethylaminopyridine ligand, there was no evidence for replacement of the amidine ligand after two months, thus establishing that the piperidinylamidine ligand is a robust ligand. This chemistry offers promise as a suitable means for preparing isomerically pure conjugated *fac*-[^{99m}Tc(CO)$_3$L]$^{n\pm}$ imaging agents, including conjugates with known bioactive heterocyclic amines.

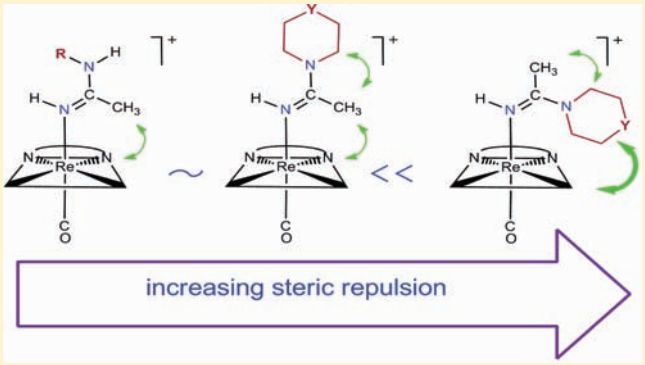

INTRODUCTION

Owing to the many ideal properties of the *fac*-[M^{I}(CO)$_3$] core in radiopharmaceuticals, *fac*-[M^{I}(CO)$_3$L]^n (M = various isotopes of Tc and Re) complexes have recently been receiving much attention.[1−7] Some *fac*-[^{99m}Tc^{I}(CO)$_3$L]^n imaging agents have undergone evaluation in humans,[8,9] and *fac*-[$^{186/188}$Re^{I}(CO)$_3$L]^n agents are emerging as being among the most promising radionuclides for therapeutic applications.[2,10,11] At present, great interest surrounds the concept of combining ^{99m}Tc and $^{186/188}$Re with biomolecules in order to produce selective targeting agents.[5,6,11−17] *fac*-[Re^{I}(CO)$_3$L]^n complexes prepared with natural-abundance rhenium are excellent models for the short-lived *fac*-[M^{I}(CO)$_3$L]^n radiopharmaceuticals and are almost nonradioactive. Thus, the investigation of *fac*-[Re^{I}(CO)$_3$L]^n complexes both aids in interpreting the chemistry of the radiopharmaceuticals and offers the potential for the discovery of new chemistry, some of which could be applied to radiopharmaceutical development.[18,19]

Our objectives are aimed at expanding the known chemistry of complexes with the *fac*-[Re^{I}(CO)$_3$] core.[7,20,21] Syntheses in aqueous media carried out with the commonly used precursor, aqueous *fac*-[Re^{I}(CO)$_3$(H$_2$O)$_3$]$^+$,[22] have some limitations.[23] Thus, we have recently investigated the suitability of *fac*-[Re(CO)$_3$(CH$_3$CN)$_3$]X (X = PF$_6$ or BF$_4$) as a precursor for the synthesis of new complexes in organic solvents.[23] Treatment of *fac*-[Re(CO)$_3$(CH$_3$CN)$_3$]X with bidentate aromatic sp^2 N-donor bipyridine-type L in either acetonitrile or benzene as a solvent produced the desired *fac*-[Re(CO)$_3$(L)(CH$_3$CN)]X complexes in excellent yield [e.g., when L = 2,2′-bipyridine (bipy) or a dimethyl-2,2′-bipyridine (Me$_2$bipy), Scheme 1].[24] However,

Received: March 24, 2012
Published: June 12, 2012

   dx.doi.org/10.1021/ic300625n | *Inorg. Chem.* 2012, 51, 7271−7283

Scheme 1. General Reaction Scheme for the Synthesis of $[Re(CO)_3(L)(CH_3CN)]^+$ Starting Material[24] and for the Formation of $[Re(CO)_3(Me_2bipy)(HNC(CH_3)OCH_3)]^+$ (Iminoether) Complexes[23]

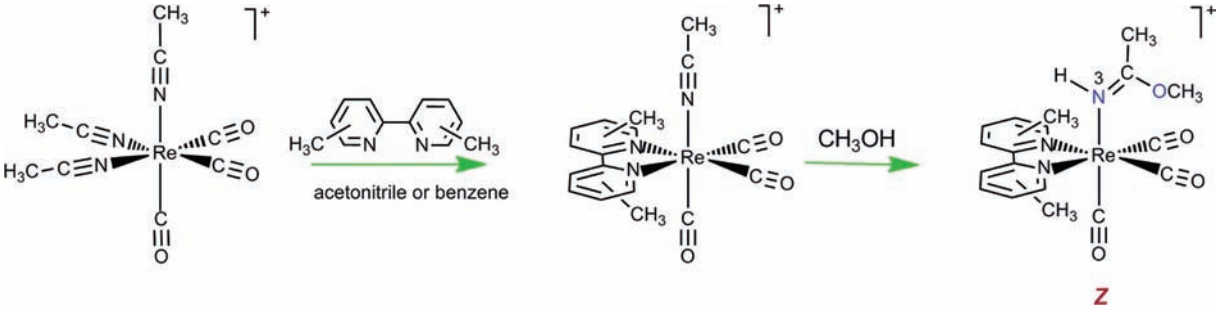

a recent study revealed that reactions to form these complexes in methanol instead led to the addition of solvent to bound acetonitrile, forming iminoether complexes, *fac*-$[Re(CO)_3(Me_2bipy)(HNC(CH_3)OCH_3)]BF_4$.[23] The original acetonitrile carbon with a triple bond to the rhenium-bound nitrogen (N3) is converted in the reaction to an iminoether carbon (C_{ie}), and N3 adds a proton and rehybridizes from sp to sp^2 (Scheme 1). The C_{ie}–N3 bond has double-bond character, and the iminoether ligand potentially can have *E* and *Z* configurations. However, the *Z* isomer (Scheme 1) is favored exclusively because the axial iminoether ligand steric repulsions with the equatorial ligands (the two CO's and the Me_2bipy) are lower for the *Z* configuration than for the *E* configuration.[23]

The reactions of *fac*-$[Re(CO)_3(5,5'\text{-}Me_2bipy)(CH_3CN)]^+$ (**1**) with alcohols to form iminoethers were slow.[23] On the other hand, the related reactions of primary amines with **1** to form amidine complexes, *fac*-$[Re(CO)_3(5,5'\text{-}Me_2bipy)(HNC(CH_3)\text{-}NHR)]^+$, were more rapid.[25] However, these amidine complexes exist as mixtures of isomers. In the $HNC(CH_3)NHR$ ligands, both C–N bonds involving the amidine carbon (C_{am}), C_{am}–N3 and C_{am}–N4, have double-bond character. This situation raises the possibility that four configurations (*E*, *E*′, *Z*, and *Z*′) of the amidine ligands could exist (Figure 1). In fact, three configurations (*E*, *E*′, and *Z*) were found.[25] The isomers are named using these configurations. As illustrated and discussed below, steric effects strongly influence the relative abundance of the isomers.

The amidine group, such as that present in *fac*-$[Re(CO)_3(5,5'\text{-}Me_2bipy)(HNC(CH_3)NHR)]BF_4$ complexes,[25] has the potential to serve as a linking group in the conjugation of the *fac*-$[M(CO)_3]^+$ core (M = ^{99m}Tc and $^{186/188}$Re radionuclides) with biomedical targeting moieties. The nitrogen donor group in amidine (and iminoether) ligands is superbasic.[23,25] However, the finding of isomers of these complexes (Figure 1) complicates the development of agents useful for biomedical imaging. Therefore, we now explore amidine ligands with a C_2-symmetrical NR_2 substituent in place of the NHR substituent. This change eliminates the possibility of two configurations about the C_{am}–N4 bond, restricting the number of conceivable isomers to two (with *E* or *Z* configurations about the C_{am}–N3 bond). Furthermore, we expected that a large difference in substituent bulk (NR_2 vs CH_3) on C_{am} should favor the *E* isomer exclusively.

We chose C_2-symmetrical saturated heterocyclic secondary amines in our synthetic strategy because many related symmetric heterocyclic amine derivatives are present in ^{99m}Tc and $^{186/188}$Re agents[13,26–31] and in successful drugs.[31,32] Because their use as ubiquitous building blocks in the synthesis of pharmaceuticals[31] has provided information on the synthesis and properties of such

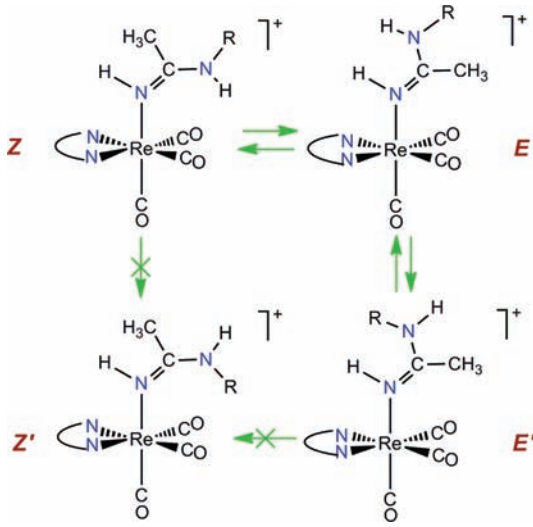

Figure 1. The four conceivable $[Re(CO)_3(5,5'\text{-}Me_2bipy)HNC(CH_3)\text{-}NHR)]^+$ isomers, in which N–N denotes the 5,5′-Me_2bipy ligand. The isomers with the *E*′ and *Z* configurations are typically abundant. The isomer with the *Z*′ configuration is unstable and not observed.[25] The isomer with the *E* configuration is known, but its abundance is usually too low to allow detection. However, as illustrated here, the pathway between the *E*′ and *Z* configurations undoubtedly passes through the *E* configuration and not the *Z*′ configuration.

amines, these amines are particularly desirable candidates for study. Indeed, a modified arylpiperazine was employed in one of the earliest examples of a *fac*-$[^{99m}Tc(CO)_3]^+$-containing agent linked to a targeting biomolecule.[13] All of the new complexes discussed below have the facial geometry, and thus from this point onward we omit the *fac* designation when discussing specific compounds.

EXPERIMENTAL SECTION

Starting Materials. $Re(CO)_5Br$ was synthesized as described in the literature.[33] $Re_2(CO)_{10}$, 5,5′-dimethyl-2,2′-bipyridine (5,5′-Me_2bipy), 6,6′-dimethyl-2,2′-bipyridine (6,6′-Me_2bipy), piperidine, homopiperidine, heptamethyleneimine, morpholine, piperazine, and $AgBF_4$ were obtained from Aldrich. $[Re(CO)_3(CH_3CN)_3]BF_4$ (prepared by a slight modification of a known procedure[34]) was used to prepare $[Re(CO)_3(5,5'\text{- or }6,6'\text{-}Me_2bipy)(CH_3CN)]BF_4$.[24]

NMR Measurements. ^{1}H NMR spectra were recorded on a 400 MHz Bruker spectrometer. Peak positions are relative to TMS or to the solvent residual peak, with TMS as a reference. All NMR data were processed with TopSpin and Mestre-C software.

X-Ray Data Collection and Structure Determination. Intensity data were collected at low temperature on a Nonius Kappa CCD diffractometer fitted with an Oxford Cryostream cooler with graphite-

dx.doi.org/10.1021/ic300625n | Inorg. Chem. 2012, 51, 7271–7283

Table 1. Crystal Data and Structural Refinement for Complexes Having the General Formula $[Re(CO)_3(5,5'\text{-}Me_2bipy)(HNC(CH_3)N(CH_2CH_2)_2Y)]BF_4$

Y =	CH_2	$(CH_2)_2$	$(CH_2)_3$	NH	O
complex	**3**	**4**	**5**	**6**	**7**
empirical formula	$C_{22}H_{26}N_4O_3Re{\cdot}BF_4$	$C_{23}H_{28}N_4O_3Re{\cdot}0.95(BF_4){\cdot}0.05(Br)$	$C_{24}H_{30}N_4O_3Re{\cdot}0.96(BF_4){\cdot}0.04(Br)$	$C_{21}H_{25}N_5O_3Re{\cdot}BF_4$	$C_{21}H_{24}N_4O_4Re{\cdot}BF_4$
fw	667.48	681.16	695.50	668.47	669.45
cryst system	monoclinic	monoclinic	monoclinic	monoclinic	monoclinic
space group	$P2_1/n$	$P2_1/n$	$P2_1/n$	$P2_1/n$	$P2_1/n$
a (Å)	11.4576(10)	13.3550(15)	13.7247 (14)	11.6155(10)	11.3847(9)
b (Å)	13.4757(15)	13.2081(14)	11.1284 (10)	12.9640(14)	13.3112(10)
c (Å)	15.9875(15)	14.7562(18)	18.141 (2)	15.8176(11)	15.7988(15)
β (deg)	97.502(5)	105.347(6)	109.392 (3)	97.341(6)	97.843(6)
V (Å^3)	2447.3(4)	2510.1(5)	2613.6 (5)	2362.3(4)	2371.8(3)
T (K)	200	150	95	95	90
Z	4	4	4	4	4
ρ_{calcd} (Mg/m^3)	1.812	1.802	1.768	1.880	1.875
abs coeff (mm^{-1})	5.03	4.98	4.78	5.21	5.19
$2\theta_{max}$ (deg)	60.2	61.0	72.6	68.4	70.0
R $[I > 2\sigma(I)]^a$	0.032	0.032	0.029	0.032	0.033
wR2^b	0.073	0.075	0.060	0.067	0.075
w scheme d, e	0.0315, 2.4602	0.0343, 3.5449	0.0230, 1.6351	0.0252, 1.6969	0.0354, 0
data/param	7180/323	7045/344	12259/345	9257/326	10062/323
res. dens (eÅ^{-3})	1.23, −1.23	1.08, −1.85	1.16, −1.54	1.37, −1.72	1.46, −1.70

$^aR = (\sum||F_o| - |F_c||)/\sum|F_o|$. ^{b}wR2 = $[\sum[w(F_o^2 - F_c^2)^2]/\sum[w(F_o^2)^2]]^{1/2}$, in which $w = 1/[\sigma^2(F_o^2) + (dP)^2 + (eP)]$ and $P = (F_o^2 + 2F_c^2)/3$.

Table 2. Crystal Data and Structural Refinement for Complexes Having the General Formula $[Re(CO)_3(6,6'\text{-}Me_2bipy)(HNC(CH_3)N(CH_2CH_2)_2Y)]BF_4$

Y =	CH_2	$(CH_2)_2$	$(CH_2)_3$	NH	O
complex	**8**	**9**	**10**	**11**	**12**
empirical formula	$C_{22}H_{26}N_4O_3Re{\cdot}BF_4$	$C_{23}H_{28}N_4O_3Re{\cdot}0.97(BF4){\cdot}$ 0.03(Br)	$C_{24}H_{30}N_4O_3Re{\cdot}BF_4$	$C_{21}H_{25}N_5O_3Re{\cdot}BF_4$	$C_{21}H_{24}N_4O_4Re{\cdot}BF_4$
fw	667.48	681.31	695.53	668.47	669.45
cryst system	monoclinic	monoclinic	monoclinic	monoclinic	monoclinic
space group	$P2_1/n$	$P2_1/n$	$P2_1/c$	$P2_1/n$	$P2_1/n$
a (Å)	8.9242(5)	11.4040(10)	12.5348(10)	12.401(2)	15.6441(15)
b (Å)	21.862(2)	17.724(2)	10.8431(9)	14.221(3)	9.3838(10)
c (Å)	12.3282(10)	12.3056(11)	19.692(2)	13.630(2)	16.1555(12)
β (deg)	95.358(4)	98.914(5)	105.942(4)	100.750(9)	91.294(4)
V (Å^3)	2394.7(3)	2457.2(4)	2573.5(4)	2361.5(7)	2371.0(4)
T (K)	90	100	90	95	90
Z	4	4	4	4	4
ρ_{calcd} (Mg/m^3)	1.851	1.842	1.795	1.880	1.875
abs coeff (mm^{-1})	5.14	5.05	4.79	5.21	5.19
$2\theta_{max}$ (deg)	72.0	69.8	68.0	65.2	71.4
R $[I > 2\sigma(I)]^a$	0.031	0.031	0.030	0.037	0.029
wR2^b	0.074	0.068	0.070	0.097	0.069
w scheme d, e	0.0349, 0	0.0271, 2.2079	0.0307, 2.8985	0.0575,0.7244	0.0349, 1.1307
data/param	10749/323	10050/333	9861/388	8537/326	10909/323
res. dens (eÅ^{-3})	1.59, −2.07	1.35, −1.99	1.83, −1.58	4.45, −2.55	2.22, −1.69

$^aR = (\sum||F_o| - |F_c||)/\sum|F_o|$. ^{b}wR2 = $[\sum[w(F_o^2 - F_c^2)^2]/\sum[w(F_o^2)^2]]^{1/2}$, in which $w = 1/[\sigma^2(F_o^2) + (dP)^2 + (eP)]$ and $P = (F_o^2 + 2F_c^2)/3$.

monochromated Mo Kα (λ = 0.71073 Å) radiation. Data reduction included absorption corrections using the multiscan method, with HKL SCALEPACK.[35] All X-ray structures were determined by direct methods and difference Fourier techniques and refined by full-matrix least-squares by using SHELXL-97.[36] All non-hydrogen atoms were refined anisotropically. All H atoms were visible in difference maps but were placed in idealized positions, except for N−H hydrogen atoms, for which coordinates were refined. A torsional parameter was refined for each methyl group. For compounds **4**, **5**, and **9**, the BF_4^- site was shared by a few percent bromide, and the occupancies of the two anions were constrained to sum to unity in the refinement. In compound **10**, the BF_4^- is disordered into two orientations and the eight-membered ring is disordered into two conformations. The occupancies refined to 0.891(5):0.109(5) for the anion and 0.521(6):0.479(6) for the eight-membered ring. Crystal data and details of refinements are listed in Tables 1 and 2.

General Synthesis of Amidine Complexes. An acetonitrile solution (6 mL) of $[Re(CO)_3(5,5'\text{-}Me_2bipy)(CH_3CN)]BF_4$ (**1**) or $[Re(CO)_3(6,6'\text{-}Me_2bipy)(CH_3CN)]BF_4$ (**2**) (40 mg, 0.06 mmol) was treated with an amine (0.60 mmol), and the reaction mixture was stirred at room temperature for 30 min or as specified. The volume was reduced to ∼1 mL by rotary evaporation. The addition of diethyl ether to the point of cloudiness (∼10−200 mL) produced a yellow crystalline material that was collected on a filter, washed with diethyl ether, and dried. ^{1}H NMR spectra that were recorded both immediately upon

dx.doi.org/10.1021/ic300625n | Inorg. Chem. 2012, 51, 7271−7283

dissolution of products **3**−**12** and also subsequently showed signals for only one isomer.

The ^{1}H NMR spectrum of all crystals described below was identical to that of the product obtained by this procedure. In order to study the progress of the amidine formation reactions, a 10 mM solution of **1** or **2** was prepared in 600 μL of acetonitrile-d_3. We refer to such a solution as the 10 mM solution. An excess of amine (100 mM) was added to the 10 mM solution, and the reaction was monitored by NMR spectroscopy. In all cases, the only signals observed for products were those expected from the isolated products.

Synthesis of [Re(CO)$_3$(5,5′-Me$_2$bipy)(HNC(CH$_3$)N-(CH$_2$CH$_2$)$_2$CH$_2$)]BF$_4$ (3). The use of this general method in the reaction of **1** with piperidine (59 μL, 0.60 mmol) afforded 30 mg (74% yield) of yellow crystalline material. ^{1}H NMR signals (ppm) in acetonitrile-d_3: 8.85 (s, 2H, H6/6′), 8.26 (d, J = 8.4 Hz, 2H, H3/3′), 8.04 (d, J = 8.4 Hz, 2H, H4/4′), 4.78 (b, 1H, NH), 3.01 (m, 4H, 2CH$_2$), 2.48 (s, 6H, 5/5′-2CH$_3$), 2.10 (s, 3H, CCH$_3$), 1.48 (m, 2H, CH$_2$), 1.28 (m, 4H, 2CH$_2$).

X-ray quality crystals of **3** (*E* isomer) were produced upon slow evaporation of a solution of the crystalline material (5 mg/6 mL) in a 1:5 (v/v) mixture of acetonitrile/diethyl ether. The ^{1}H NMR spectrum of the crystals dissolved in acetonitrile-d_3 was identical to that of the bulk product.

Monitoring the progress of the reaction of **1** with piperidine (5.9 μL) as described above indicated that no signals for **1** remained after 5 min, and signals for **3** were the only product signals present.

Synthesis of [Re(CO)$_3$(5,5′-Me$_2$bipy)(HNC(CH$_3$)N-(CH$_2$CH$_2$)$_2$(CH$_2$)$_2$)]BF$_4$ (4). The use of the general method in the reaction of **1** with homopiperidine (60 μL, 0.60 mmol) produced 33 mg (80% yield) of yellow crystalline material. ^{1}H NMR signals (ppm) in acetonitrile-d_3: 8.87 (s, 2H, H6/6′), 8.27 (d, J = 8.6 Hz, 2H, H3/3′), 8.05 (d, J = 8.1 Hz, 2H, H4/4′), 4.52 (b, 1H, NH), 3.30 (b, m, 2H, CH$_2$), 2.96 (b, m, 2H, CH$_2$), 2.48 (s, 6H, 5/5′-2CH$_3$), 2.10 (s, 3H, CCH$_3$), 1.46 (b, m, 2H, CH$_2$), 1.31 (b, m, 2H, CH$_2$), 1.15 (b, m, 2H, CH$_2$), 0.96 (b, m, 2H, CH$_2$).

X-ray quality crystals of **4** (*E* isomer) grew upon slow evaporation of a solution of the crystalline material (5 mg/4 mL) in a 1:3 (v/v) mixture of acetonitrile/diethyl ether. The ^{1}H NMR spectrum of the crystals dissolved in acetonitrile-d_3 was identical to that of the bulk product.

Monitoring the progress of the reaction of **1** with homopiperidine (6 μL) as described above indicated that no signals for **1** remained after ∼8 min.

Synthesis of [Re(CO)$_3$(5,5′-Me$_2$bipy)(HNC(CH$_3$)N-(CH$_2$CH$_2$)$_2$(CH$_2$)$_3$)]BF$_4$ (5). The use of the general method in the reaction of **1** with heptamethyleneimine (76 μL, 0.60 mmol), but stirring for 8 h, yielded 13 mg (32%) of yellow crystalline material. ^{1}H NMR signals (ppm) in acetonitrile-d_3: 8.87 (s, 2H, H6/6′), 8.27 (d, J = 8.3 Hz, 2H, H3/3′), 8.04 (d, J = 8.0 Hz, 2H, H4/4′), 4.49 (b 1H, NH), 3.25 (b, 2H, CH$_2$), 3.05 (b, 2H, CH$_2$), 2.48 (s, 6H, 5/5′-2CH$_3$), 2.12 (s, 3H, CCH$_3$), 1.50 (b, m, 2H, CH$_2$), 1.39 (b, m, 2H, CH$_2$), 1.18 (b, m, 2H, CH$_2$), 0.96 (b, m, 2H, CH$_2$), 0.71 (b, m, 2H, CH$_2$).

X-ray quality crystals of **5** (*E* isomer) grew upon slow evaporation of a solution of the crystalline material (10 mg/∼200 mL) in a 1:200 (v/v) mixture of acetonitrile/diethyl ether. The ^{1}H NMR spectrum of the crystals dissolved in acetonitrile-d_3 was identical to that of the bulk product.

Monitoring the progress of the reaction of **1** with heptamethyleneimine (7.6 μL) as described above indicated that no signals for **1** remained after 6 h.

Synthesis of [Re(CO)$_3$(5,5′-Me$_2$bipy)(HNC(CH$_3$)N-(CH$_2$CH$_2$)$_2$NH)]BF$_4$ (6). The general synthetic reaction of **1** with piperazine (52 mg, 0.60 mmol) yielded 34 mg (84%) of yellow crystalline material. ^{1}H NMR signals (ppm) in acetonitrile-d_3: 8.85 (s, 2H, H6/6′), 8.26 (d, J = 8.4 Hz, 2H, H3/3′), 8.04 (d, J = 8.4 Hz, 2H, H4/4′), 4.84 (b, 1H, NH), 2.95 (m, 4H, 2CH$_2$), 2.53 (m, 4H, 2CH$_2$), 2.48 (s, 6H, 5/5′-2CH$_3$), 2.12 (s, 3H, CCH$_3$).

X-ray quality crystals of **6** (*E* isomer) formed upon slow evaporation of a 16 mL solution of the crystalline material (5 mg) in a 1:15 (v/v) mixture of acetonitrile/diethyl ether. The ^{1}H NMR spectrum of the crystals dissolved in acetonitrile-d_3 was identical to that of the bulk product.

Monitoring the progress of the reaction of **1** with piperazine (5.2 mg) as described above indicated that no signals for **1** remained after 20 min.

Synthesis of [Re(CO)$_3$(5,5′-Me$_2$bipy)(HNC(CH$_3$)N-(CH$_2$CH$_2$)$_2$O)]BF$_4$ (7). The general synthetic reaction of **1** with morpholine (53 μL, 0.60 mmol; stirring time, 6 h) yielded 33 mg (83%) of yellow crystalline material. ^{1}H NMR signals (ppm) in acetonitrile-d_3: 8.85 (s, 2H, H6/6′), 8.26 (d, J = 8.4 Hz, 2H, H3/3′), 8.05 (d, J = 8.1 Hz, 2H, H4/4′), 4.94 (b, 1H, NH), 3.45 (m, 2H, CH$_2$), 3.00 (m, 2H, CH$_2$), 2.48 (s, 6H, 5/5′-2CH$_3$), 2.14 (s, 3H, CCH$_3$).

X-ray quality crystals of **7** (*E* isomer) grew upon slow evaporation of a 4 mL solution of the crystalline material (5 mg) in a 1:3 (v/v) mixture of acetonitrile/diethyl ether. The ^{1}H NMR spectrum of the crystals dissolved in acetonitrile-d_3 was identical to that of the bulk product.

Monitoring the progress of the reaction of **1** with morpholine (5.3 μL) as described above indicated that no signals for **1** remained after 4 h.

Synthesis of [Re(CO)$_3$(6,6′-Me$_2$bipy)(HNC(CH$_3$)N-(CH$_2$CH$_2$)$_2$CH$_2$)]BF$_4$ (8). The general treatment of **2** with piperidine (59 μL, 0.60 mmol) yielded 35 mg (88%) of yellow crystalline material. ^{1}H NMR signals (ppm) in acetonitrile-d_3: 8.19 (d, J = 8.1 Hz, 2H, H3/3′), 8.06 (t, J = 7.9 Hz 2H, H4/4′), 7.62 (d, J = 7.9 Hz, 2H, H5/5′), 5.14 (b, 1H, NH), 3.06 (s, 6H, 6/6′-2CH$_3$), 3.03 (overlapped m, 4H, 2CH$_2$), 1.60 (s, 3H, CCH$_3$), 1.53 (m, 2H, CH$_2$), 1.29 (m, 4H, 2CH$_2$).

X-ray quality crystals of **8** (*E* isomer) formed upon slow evaporation of a 6 mL solution of the crystalline material (5 mg) in a 1:5 (v/v) mixture of acetonitrile/diethyl ether. The ^{1}H NMR spectrum of the crystals dissolved in acetonitrile-d_3 was identical to that of the bulk product.

Monitoring the progress of the reaction of **2** with piperidine (5.9 μL) as described above indicated that no signals for **2** remained after 3 min.

Synthesis of [Re(CO)$_3$(6,6′-Me$_2$bipy)(HNC(CH$_3$)N-(CH$_2$CH$_2$)$_2$(CH$_2$)$_2$)]BF$_4$ (9). The general treatment of **2** with homopiperidine (60 μL, 0.60 mmol) yielded 32 mg (78%) of yellow crystalline material. ^{1}H NMR signals (ppm) in acetonitrile-d_3: 8.19 (d, J = 7.8 Hz, 2H, H3/3′), 8.06 (t, J = 7.9 Hz, 2H, H4/4′), 7.61 (d, J = 7.8 Hz, 2H, H5/5′), 4.90 (b, 1H, NH), 3.26 (b, m, 2H, CH$_2$), 3.07 (s, 6H, 6/6′-2CH$_3$), 3.04 (overlapped m, 2H, CH$_2$), 1.62 (s, 3H, CCH$_3$), 1.44 (b, m, 2H, CH$_2$), 1.38 (b, m, 2H, CH$_2$), 1.32 (b, m, 2H, CH$_2$), 1.11 (b, m, 2H, CH$_2$).

X-ray quality crystals of **9** (*E* isomer) grew upon slow evaporation of a 5 mL solution of the crystalline material (5 mg) in a 1:4 (v/v) mixture of acetonitrile/diethyl ether. The ^{1}H NMR spectrum of the crystals dissolved in acetonitrile-d_3 was identical to that of the bulk product.

Monitoring the progress of the reaction of **2** with homopiperidine (6 μL) as described above indicated that no signals for **2** remained after ∼4.5 min.

Synthesis of [Re(CO)$_3$(6,6′-Me$_2$bipy)(HNC(CH$_3$)N-(CH$_2$CH$_2$)$_2$(CH$_2$)$_3$)]BF$_4$ (10). The general treatment of **2** with heptamethyleneimine (76 μL, 0.60 mmol) afforded 15 mg (35%) of yellow crystalline material. ^{1}H NMR signals (ppm) in acetonitrile-d_3: 8.19 (d, J = 8.1 Hz, 2H, H3/3′), 8.07 (t, J = 7.9 Hz, 2H, H4/4′), 7.63 (d, J = 7.7 Hz, 2H, H5/5′), 4.82 (b, 1H, NH), 3.23 (b, m, 2H, CH$_2$), 3.16 (b, m, 2H, CH$_2$), 3.07 (s, 6H, 6/6′-2CH$_3$), 1.66 (s, 3H, CCH$_3$), 1.49 (b, m, 2H, CH$_2$), 1.42 (b, m, 2H, CH$_2$), 1.32 (b, m, 2H, CH$_2$), 1.21 (b, m, 2H, CH$_2$), 0.92 (b, m, 2H, CH$_2$).

X-ray quality crystals of **10** (*E* isomer) formed upon slow evaporation of a solution of the crystalline material (5 mg/16 mL) in a 1:15 (v/v) mixture of acetonitrile/diethyl ether. The ^{1}H NMR spectrum of the crystals dissolved in acetonitrile-d_3 was identical to that of the bulk product.

Monitoring the progress of the reaction of **2** with heptamethyleneimine (7.6 μL) as described above indicated that no signals for **2** remained after 6 min.

Synthesis of [Re(CO)$_3$(6,6′-Me$_2$bipy)(HNC(CH$_3$)N-(CH$_2$CH$_2$)$_2$NH)]BF$_4$ (11). The general treatment of **2** with piperazine (52 mg, 0.60 mmol) yielded 33 mg (83%) of yellow crystalline material. ^{1}H NMR signals (ppm) in acetonitrile-d_3: 8.19 (d, J = 8.0 Hz, 2H, H3/3′), 8.07 (t, J = 7.9 Hz, 2H, H4/4′), 7.62 (d, J = 7.7 Hz, 2H, H5/5′), 5.18 (b, 1H, NH), 3.05 (s, 6H, 6/6′-2CH$_3$), 2.96 (m, 4H, 2CH$_2$), 2.53 (m, 4H, 2CH$_2$), 1.63 (s, 3H, CCH$_3$).

dx.doi.org/10.1021/ic300625n | *Inorg. Chem.* 2012, 51, 7271−7283

X-ray quality crystals of **11** (*E* isomer) grew upon slow evaporation of a solution of the crystalline material (5 mg/5 mL) in a 1:4 (v/v) mixture of acetonitrile/diethyl ether. The ^{1}H NMR spectrum of the crystals dissolved in acetonitrile-d_3 was identical to that of the bulk product.

Monitoring the progress of the reaction of **2** with piperazine (5.1 mg) as described above indicated that no signals for **2** remained after 3 min.

Synthesis of [Re(CO)$_3$(6,6′-Me$_2$bipy)(HNC(CH$_3$)N(CH$_2$CH$_2$)$_2$O)]BF$_4$ (12). The general treatment of **2** with morpholine (53 μL, 0.60 mmol) (stirring time, 1 h) afforded 36 mg (90%) of yellow crystalline material. ^{1}H NMR signals (ppm) in acetonitrile-d_3: 8.19 (d, J = 7.9 Hz, 2H, H3/3′), 8.07 (t, J = 7.9 Hz, 2H, H4/4′), 7.62 (d, J = 7.7 Hz, 2H, H5/5′), 5.30 (b, 1H, NH), 3.45 (m, 4H, 2CH$_2$), 3.05 (s, 6H, 6/6′-2CH$_3$), 3.01 (m, 4H, 2CH$_2$), 1.66 (s, 3H, CCH$_3$).

X-ray quality crystals of **12** (*E* isomer) grew upon slow evaporation of a solution of the crystalline material (5 mg/4 mL) in a 1:3 (v/v) mixture of acetonitrile/diethyl ether. The ^{1}H NMR spectrum of the crystals dissolved in acetonitrile-d_3 was identical to that of the bulk product.

Monitoring the progress of the reaction of **2** with morpholine (5.3 μL) as described above indicated that no signals for **2** remained after 30 min.

Challenge Reactions. A 5 mM solution of [Re(CO)$_3$(5,5′-Me$_2$bipy)(HNC(CH$_3$)N(CH$_2$CH$_2$)$_2$CH$_2$)]BF$_4$ (**3**) in acetonitrile-d_3 (600 μL) was treated with a 5-fold excess of 4-dimethylaminopyridine (2.0 mg, 25 mM), and the solution was monitored over time by ^{1}H NMR spectroscopy. A similar experiment was conducted in CDCl$_3$.

RESULTS AND DISCUSSION

Synthesis. Treatment of [Re(CO)$_3$(L)(CH$_3$CN)]BF$_4$ (L = 5,5′-Me$_2$bipy (**1**), and 6,6′-Me$_2$bipy (**2**)) with heterocyclic amines in acetonitrile at room temperature afforded good yields (usually greater than 70%) of amidine complexes of the general formula [Re(CO)$_3$(L)(HNC(CH$_3$)N(CH$_2$CH$_2$)$_2$Y)]BF$_4$ (L = 5,5′-Me$_2$bipy or 6,6′-Me$_2$bipy; Y = CH$_2$, (CH$_2$)$_2$, (CH$_2$)$_3$, NH, or O), as illustrated in Figure 2. ^{1}H NMR spectroscopic studies and

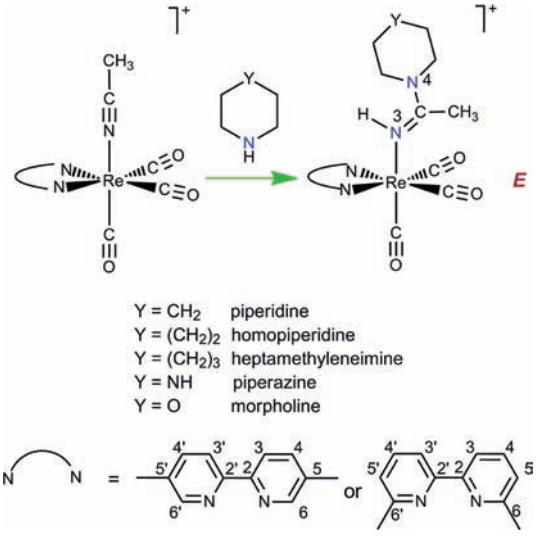

Figure 2. Reactions forming [Re(CO)$_3$(L)(HNC(CH$_3$)N(CH$_2$CH$_2$)$_2$Y)]$^+$ complexes observed upon treatment of [Re(CO)$_3$(L)(CH$_3$CN)]$^+$ complexes with heterocyclic amines (HN(CH$_2$CH$_2$)$_2$Y) in acetonitrile at 25 °C.

structural characterization by single-crystal X-ray crystallography (see below) show that the reactions with cyclic amines form only one isomer (*E*) of the new amidine complexes. Reactions are often rapid at ambient temperature (≤3 min for complete reaction). Because the greater reactivity of [Re(CO)$_3$(6,6′-Me$_2$bipy)(CH$_3$CN)]BF$_4$ (**2**) than that of [Re(CO)$_3$(5,5′-Me$_2$bipy)(CH$_3$CN)]BF$_4$ (**1**) with a given amine is best understood after a discussion of structural and spectroscopic results, we shall return to the topic of reaction times later.

Structural Results. Summarized in Tables 1 and 2 are the crystal data and details of the structural refinement for complexes **3**−**12**, having the general formula [Re(CO)$_3$(L)(HNC(CH$_3$)N(CH$_2$CH$_2$)$_2$Y)]BF$_4$ (L = 5,5′-Me$_2$bipy or 6,6′-Me$_2$bipy; Y = CH$_2$, (CH$_2$)$_2$, (CH$_2$)$_3$, NH, or O). Figures 3 and 4 show the ORTEP plots of the cations in complexes **3**−**12**, together with the numbering scheme used to describe the solid-state data. All complexes have a pseudo-octahedral structure, in which the three carbonyl ligands are coordinated facially. The remaining three coordination sites are occupied by the two nitrogen atoms of L and by one nitrogen atom of the neutral monodentate amidine ligand having the *E* configuration. Ni(II) amidine complexes formed upon the addition of secondary amines to coordinated acetonitrile have the *E* configuration in the solid state.[38,39]

The Re−C bond distances (not shown) of the two CO groups cis to the amidine ligand are generally not significantly different from the one trans to it in all complexes (**3**−**12**). All of the [Re(CO)$_3$(5,5′-Me$_2$bipy)(HNC(CH$_3$)N(CH$_2$CH$_2$)$_2$Y)]BF$_4$ complexes (**3**−**7**) show Re−N bond lengths (Table 3) comparable to the typical Re sp^2 nitrogen bond length, typically ranging from 2.14 to 2.18 Å.[22] This result is consistent with the structural results for the recent monodentate amidine complexes of Re^I with primary amines.[25] As found for the iminoether complexes, in which the Re−N3 bond lengths found for [Re(CO)$_3$(5,5′-Me$_2$bipy)(HNC(CH$_3$)OCH$_3$)]BF$_4$ (2.1860(18) Å) and [Re(CO)$_3$(6,6′-Me$_2$bipy)(HNC(CH$_3$)OCH$_3$)]BF$_4$ (2.175(3) Å) were not significantly different,[23] the Re−N3 bond lengths are quite similar for complexes **3**−**12**. These bond lengths appear to be very slightly longer for the 6,6′-Me$_2$bipy complexes (range 2.1848(18)−2.193(2), mean 2.190 Å) than for the 5,5′-Me$_2$bipy complexes (range 2.178(3)−2.1806(18), mean 2.179 Å).

The recent study of *fac*-[Re(CO)$_3$(L)(HNC(CH$_3$)OCH$_3$)]BF$_4$ complexes revealed that the Re−N bond lengths in the equatorial plane were significantly longer for L = 6,6′-Me$_2$bipy than for L = 5,5′-Me$_2$bipy.[23] These examples of a slight Re−N bond lengthening were attributed to the distorted nature of the 6,6′-Me$_2$bipy ligand as a result of the close proximity of the two methyl substituents to the equatorial carbonyl groups. A comparison of the equatorial Re−N bond lengths (Tables 3 and 4) of all five [Re(CO)$_3$(6,6′-Me$_2$bipy)(HNC(CH$_3$)N(CH$_2$CH$_2$)$_2$Y)]BF$_4$ complexes (**8**−**12**) with those of the corresponding five [Re(CO)$_3$(5,5′-Me$_2$bipy)(HNC(CH$_3$)N(CH$_2$CH$_2$)$_2$Y)]BF$_4$ complexes (**3**−**7**) reveals that only some bonds in the 6,6′-Me$_2$bipy complexes are slightly longer by criteria of statistical significance. However, as for the Re−N3 axial distances, the equatorial Re−N(Me$_2$bipy) distances appear to be on average very slightly longer for the 6,6′-Me$_2$bipy complexes (range 2.194(2)−2.213(2), mean 2.206 Å) than for the 5,5′-Me$_2$bipy complexes (range 2.168(3)−2.194(2), mean 2.179 Å). Thus, the more extensive solid-state results for complexes **3**−**12** now available indicate that the 6,6′-methyl groups in **8**−**12** affect the equatorial Re−N bond distances only slightly.

In all but one of the new complexes, the amidine ligand has a similar orientation (specified by the projection onto the equatorial plane of the amidine plane defined by the N3, C16, and N4 atoms). In this orientation, the amidine plane bisects the two N−Re−C angles in the equatorial plane. In [Re(CO)$_3$(5,5′-Me$_2$bipy)(HNC(CH$_3$)N(CH$_2$CH$_2$)$_2$(CH$_2$)$_2$)]BF$_4$ (**4**), the amidine plane orientation is different: it is rotated by about 65°, with the methyl group almost directly above one carbonyl ligand.

dx.doi.org/10.1021/ic300625n | Inorg. Chem. 2012, 51, 7271−7283

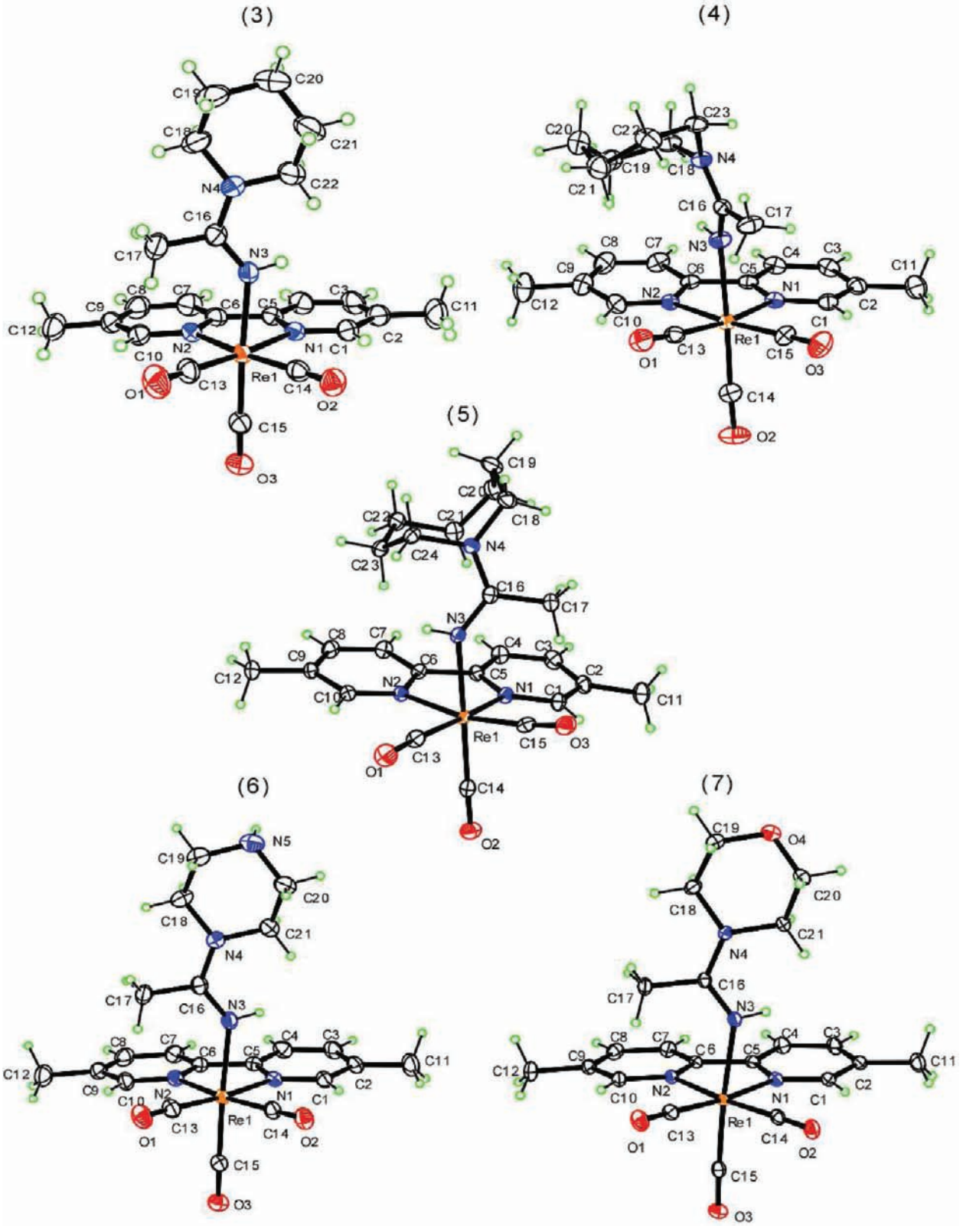

Figure 3. ORTEP plots of the cations in $[Re(CO)_3(5,5'\text{-}Me_2bipy)(HNC(CH_3)N(CH_2CH_2)_2CH_2)]BF_4$ (**3**), $[Re(CO)_3(5,5'\text{-}Me_2bipy)(HNC(CH_3)N(CH_2CH_2)_2(CH_2)_2)]BF_4$ (**4**), $[Re(CO)_3(5,5'\text{-}Me_2bipy)(HNC(CH_3)N(CH_2CH_2)_2(CH_2)_3)]BF_4$ (**5**), $[Re(CO)_3(5,5'\text{-}Me_2bipy)(HNC(CH_3)N(CH_2CH_2)_2NH)]BF_4$ (**6**), and $[Re(CO)_3(5,5'\text{-}Me_2bipy)(HNC(CH_3)N(CH_2CH_2)_2O)]BF_4$ (**7**). Thermal ellipsoids are drawn with 50% probability.

However, in solution, there is no evidence for this difference in orientation, as the ^1H NMR signals of **4** have chemical shifts similar to those of other $[Re(CO)_3(5,5'\text{-}Me_2bipy(HNC(CH_3)N(CH_2CH_2)_2Y)]BF_4$ complexes (**3**, **5**, **6**, **7**). The different orientation in **4** is thus attributed to subtle packing effects. Furthermore, the structures of most of the complexes in this and previous studies lead us to conclude that the orientation of the amidine and iminoether ligands does not depend on the

dx.doi.org/10.1021/ic300625n | *Inorg. Chem.* 2012, 51, 7271−7283

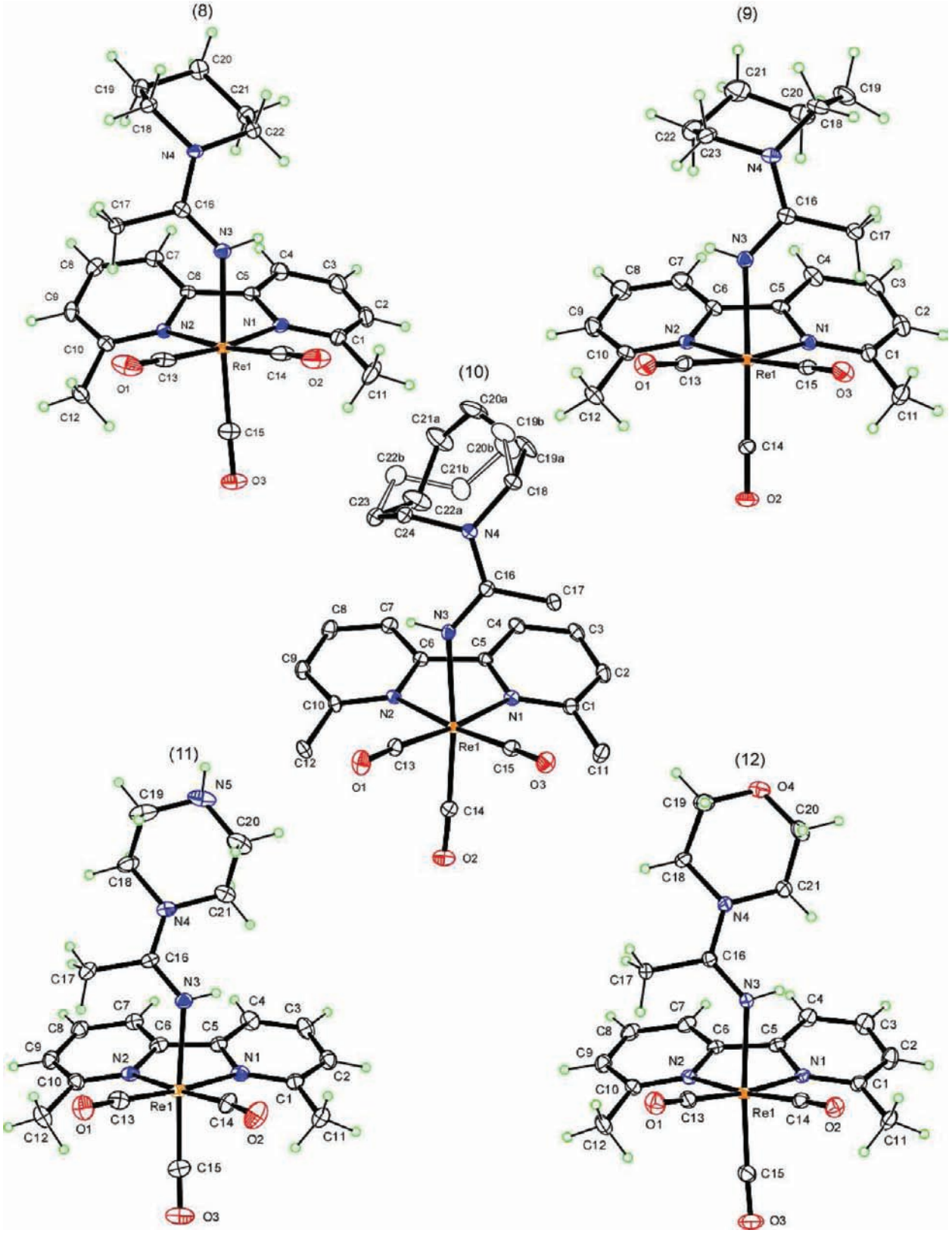

Figure 4. ORTEP plots of the cations in $[Re(CO)_3(6,6'\text{-}Me_2bipy)(HNC(CH_3)N(CH_2CH_2)_2CH_2)]BF_4$ (**8**), $[Re(CO)_3(6,6'\text{-}Me_2bipy)(HNC(CH_3)N(CH_2CH_2)_2(CH_2)_2)]BF_4$ (**9**), $[Re(CO)_3(6,6'\text{-}Me_2bipy)(HNC(CH_3)N(CH_2CH_2)_2(CH_2)_3)]BF_4$ (**10**), $[Re(CO)_3(6,6'\text{-}Me_2bipy)(HNC(CH_3)N(CH_2CH_2)_2NH)]BF_4$ (**11**), and $[Re(CO)_3(6,6'\text{-}Me_2bipy)(HNC(CH_3)N(CH_2CH_2)_2O)]BF_4$ (**12**). Thermal ellipsoids are drawn with 50% probability. For **10**, both conformations of the disordered eight-membered ring are shown, and H atoms are not illustrated, except for N−H.

substitution pattern of the bipyridine ligands (L = 5,5′-Me_2bipy or L = 6,6′-Me_2bipy) present in the equatorial plane.[23,25]

Tables 3 and 4 show that for complexes **3**−**12** the bond lengths from C_{am} (C16) to the rhenium-bound nitrogen atom (N3), and

dx.doi.org/10.1021/ic300625n | *Inorg. Chem.* 2012, 51, 7271−7283

Table 3. Selected Bond Distances (Å) and Angles (deg) for Complexes Having the General Formula $[Re(CO)_3(5,5'\text{-}Me_2bipy)(HNC(CH_3)N(CH_2CH_2)_2Y)]BF_4$

Y =	CH_2	$(CH_2)_2$	$(CH_2)_3$	NH	O
complex	**3**	**4**	**5**	**6**	**7**
		bond distances			
Re−N1	2.168(3)	2.172(3)	2.1691(18)	2.177(2)	2.177(2)
Re−N2	2.186(3)	2.173(3)	2.1823(18)	2.190(2)	2.194(2)
Re−N3	2.178(3)	2.179(3)	2.1806(18)	2.179(2)	2.178(2)
N3−C16	1.306(4)	1.310(5)	1.308(3)	1.300(4)	1.304(3)
N4−C16	1.346(5)	1.344(5)	1.346(3)	1.354(4)	1.359(3)
		bond angles			
N1−Re−N2	75.06(11)	74.58(11)	74.82(6)	75.08(8)	75.16(8)
N1−Re−N3	80.23(11)	83.44(11)	87.21(6)	79.90(9)	78.78(8)
N2−Re−N3	86.41(11)	79.02(11)	79.34(6)	86.11(9)	86.30(8)
Re−N3−H3N	113(3)	111(3)	106(2)	110(2)	110(2)
Re−N3−C16	137.4(2)	135.6(3)	136.82(15)	136.5(2)	137.03(18)
C16−N3−H3N	110(3)	110(3)	116(2)	114(2)	113(2)
N3−C16−N4	123.6(3)	122.9(3)	122.47(19)	123.3(3)	122.5(2)
N3−C16−C17	118.6(3)	118.5(3)	119.58(19)	119.2(3)	119.9(2)
N4−C16−C17	117.8(3)	118.7(3)	117.95(19)	117.4(2)	117.7(2)
C16−N4−C18	122.2(3)	121.2(3)	123.86(18)	121.8(2)	121.4(2)
C16−N4−C(n)[a]	120.3(3)[b]	122.7(3)[c]	120.44(18)[d]	120.7(2)[e]	120.1(2)[e]

[a] n varies in number according to the R group. [b] n = 22. [c] n = 23. [d] n = 24. [e] n = 21.

Table 4. Selected Bond Distances (Å) and Angles (deg) for Complexes Having the General Formula, $[Re(CO)_3(6,6'\text{-}Me_2bipy)(HNC(CH_3)N(CH_2CH_2)_2Y)]BF_4$

Y =	CH_2	$(CH_2)_2$	$(CH_2)_3$	NH	O
complex	**8**	**9**	**10**	**11**	**12**
		bond distances			
Re−N1	2.213(2)	2.203(2)	2.211(2)	2.212(3)	2.2051(19)
Re−N2	2.1984(18)	2.194(2)	2.211(2)	2.202(3)	2.2086(19)
Re−N3	2.193(2)	2.188(2)	2.190(2)	2.192(3)	2.1848(18)
N3−C16	1.307(3)	1.309(3)	1.308(3)	1.307(4)	1.307(3)
N4−C16	1.356(3)	1.350(3)	1.347(3)	1.350(4)	1.356(3)
		bond angles			
N1−Re−N2	74.29(7)	74.60(8)	74.40(8)	75.29(11)	74.90(7)
N1−Re−N3	80.26(7)	82.12(8)	83.41(8)	79.19(10)	79.35(7)
N2−Re−N3	82.97(7)	80.44(8)	79.26(8)	83.85(10)	82.00(7)
Re−N3−H3N	110(2)	110(2)	108(2)	107(3)	109(2)
Re−N3−C16	136.66(16)	135.62(19)	136.74(19)	135.4(2)	137.12(15)
C16−N3−H3N	113(2)	115(2)	115(2)	115(3)	114(2)
N3−C16−N4	123.2(2)	122.9(2)	123.0(2)	124.2(3)	122.84(19)
N3−C16−C17	119.5(2)	119.8(2)	119.2(2)	118.4(3)	119.85(19)
N4−C16−C17	117.3(2)	117.3(2)	117.8(2)	117.3(3)	117.28(19)
C16−N4−C18	122.62(19)	122.4(2)	123.2(2)	124.2(3)	122.27(18)
C16−N4−C(n)[a]	122.93(19)[b]	121.2(2)[c]	121.0(2)[d]	123.7(3)[e]	121.29(19)[e]

[a] n varies in number according to the R group. [b] n = 22. [c] n = 23. [d] n = 24. [e] n = 21.

to the remote nitrogen atom (N4), are all closer to an average sp^2 C═N bond length (~1.28 Å) than to an average sp^3 C−N bond length (~1.47 Å), as also reported for $[Re(CO)_3(5,5'\text{-}Me_2bipy)(HNC(CH_3)NHR)]BF_4$ complexes[25] and for Ni and Cu complexes.[37−39] In addition to the C16−N3 and C16−N4 bond lengths, the values of the C16−N4−C18, C16−N4−C(n), and N3−C16−N4 angles, which are all close to 120° (Tables 3 and 4), also provide evidence for electron delocalization within the amidine group, as discussed in previous reports.[23,37−40] Furthermore, the N3 hydrogen atoms in these complexes are all located in positions consistent with sp^2 rather than sp^3 hybridization for N3.

Distances that are slightly shorter for C16−N3 than for C16−N4 (Tables 3 and 4) indicate more double-bond character in the C16−N3 bond. For example, in $[Re(CO)_3(5,5'\text{-}Me_2bipy)(HNC(CH_3)N(CH_2CH_2)_2CH_2)]BF_4$ (**3**), the C16−N3 bond length is 1.306(4) Å and the C16−N4 bond length is 1.346(5) Å. Similar differences in the C16−N3 and C16−N4 bond distances reported previously for $[Re(CO)_3(5,5'\text{-}Me_2bipy)(HNC(CH_3)NHR)]BF_4$ complexes were attributed to greater double-bond character for the C16−N3 bond than for the C16−N4 bond.[25]

In the solid state, $[Re(CO)_3(5,5'\text{-}Me_2bipy)(HNC(CH_3)NHR)]BF_4$ complexes exist as the E' isomer.[25] In solutions made with polar solvents such as acetonitrile, the E' isomer equilibrated to a mixture of the E' and Z isomers. This

dx.doi.org/10.1021/ic300625n | Inorg. Chem. 2012, 51, 7271−7283

equilibration, involving sequential rotations around the C16−N4 bond (fast step forming the *E* isomer as an undetectable intermediate in polar solvents) and then around the C16−N3 bond (slow step), required several minutes.[25] The solution results are consistent with the X-ray data that indicate more double-bond character in the C16−N3 bond than in the C16−N4 bond. In solvents with low polarity, such as chloroform, abundant amounts of *E*, *E*′, and *Z* isomers were found. Two-dimensional NMR data demonstrated that the *E*′ to *E* interconversion, involving rotation around the C16−N4 bond (Figure 1), was fast. The similarity in the C16−N3 and C16−N4 bond distances in new and old amidine complexes indicates that *E* to *Z* isomer interconversion should be slow for the new amidine complexes (**3**−**12**) as well. Thus, the NMR evidence (see below) for the presence of only one isomer on dissolution of crystals containing only the *E* isomer indicates beyond doubt that this one isomer is the *E* isomer and that the *Z* isomer of the new $[Re(CO)_3(L)(HNC(CH_3)N(CH_2CH_2)_2Y)]BF_4$ complexes (**3**−**12**) is unstable. Preliminary data suggest that the rotation around the C16−N4 bond does occur and studies are planned to elucidate this process.

Steric Interaction of the Amidine Axial Ligand with the Equatorial Ligands. For amidine complexes **3**−**12**, one of the bond angles from an equatorial N atom to the axial N3 atom (N1−Re−N3 or N2−Re−N3) is always significantly greater than the other such angle. For example, in complexes **3**, **6**, **7**, **8**, **11**, and **12**, the N2−Re−N3 angle is greater than the N1−Re−N3 angle, whereas in complexes **4**, **5**, **9**, and **10**, the N1−Re−N3 angle is the larger (cf. Tables 3 and 4). The smaller N−Re−N3 angle is always the one involving the equatorial N closest to the amidine N3H group. A similar relationship was also evident between the smaller equatorial N−Re−N3 bond angle and the orientation of the N3H group of previously studied primary amidine[25] and iminoether[23] complexes, when the axial ligand was oriented in the normal way. For the new complexes, this normal orientation is shown in the Supporting Information. The reason that one N−Re−N3 bond angle is significantly larger than the other N−Re−N3 bond angle in complexes **3**−**12** is clearly because the larger angle leads to reduced repulsions between the amidine methyl group and the closest atoms of equatorial ligands.

When we began our investigations into reactions of coordinated acetonitrile in complexes with the *fac*-$[M^I(CO)_3]$ core, one initial goal was to explore the effect of increasing the steric bulk near the metal center by using the 6,6′-Me_2bipy ligand. In the first such study (involving iminoether complexes), we found that, when the iminoether was oriented in the same way, the value of the larger N−Re−N3 angle in $[Re(CO)_3(bipy)(HNC(CH_3)OCH_3)]BF_4$ was greater than the corresponding larger N−Re−N3 value in $[Re(CO)_3(6,6'\text{-}Me_2bipy)(HNC(CH_3)OCH_3)]BF_4$.[23] We hypothesized that the distortion in the 6,6′-Me_2bipy complex decreases those interactions of the axial iminoether ligand with the equatorial ligands that cause one of the two N−Re−N3 angles to be larger.

In the new complexes, the size of the larger of the two N−Re−N3 bond angles in the 5,5′-Me_2bipy complexes is greater on average than the larger bond angles in the 6,6′-Me_2bipy complexes (Tables 3 and 4 and Supporting Information). This comparison supports the hypothesis that the distortion in the 6,6′-Me_2bipy complexes decreases those axial−equatorial ligand interactions that cause one of the two N−Re−N3 angles to be larger. This apparently counterintuitive finding of smaller interactions in 6,6′-Me_2bipy complexes than in the related $[Re(CO)_3(bipy)(HNC(CH_3)OCH_3)]BF_4$ complexes can be understood by considering our structural results and those that have appeared during the course of our work.[23] In the many structures now available, the clashes between the methyl groups of the 6,6′-Me_2bipy ligand and the two equatorial CO ligands distort the 6,6′-Me_2bipy ligand and force the 6,6′-methyl groups out of the equatorial plane (defined by the C13−Re−C14 atoms) toward the axial CO. These distortions of the $Re(CO)_3$(6,6′-Me_2bipy) moiety in $[Re(CO)_3(6,6'\text{-}Me_2bipy)(HNC(CH_3)N(CH_2CH_2)_2Y)]BF_4$ amidine complexes (**8**−**12**; Figure 5 and Supporting Information) are very similar to those of the other complexes.[23,41]

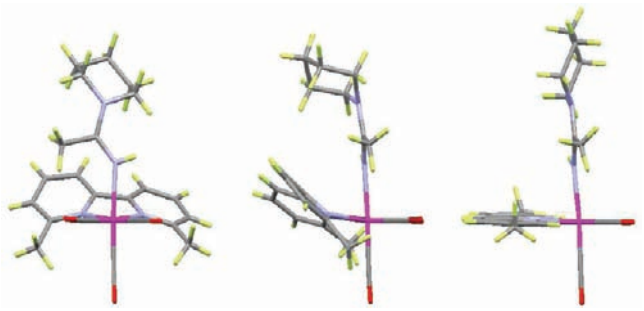

Figure 5. Views of piperidinylamidine complexes, $[Re(CO)_3(L)(HNC(CH_3)N(CH_2CH_2)_2CH_2)]BF_4$, depicted with the C13−Re−C14 equatorial plane perpendicular to the plane of the paper. Shown at *left* and *middle* are front and side views, respectively, of complex **8** with L = 6,6′-Me_2bipy. Pictured at *right* is a side view of complex **3** with L = 5,5′-Me_2bipy.

As can be seen in Figure 5, the distortion results in a tilted plane of the 6,6′-Me_2bipy ligand. To appreciate the effect of the tilting, it is convenient to view the two Me_2bipy ligands as having an interior or front side (atoms N1, C1, N2, C10) and an exterior or back side (atoms C3, C4, C7, C8), according to the numbering scheme in Figures 3 and 4. Although in the solid state the ligands are not fully symmetrical or fully planar, the front-side carbons 1 and 10 lie slightly below the equatorial plane in 6,6′-Me_2bipy complexes and lie in the equatorial plane in 5,5′-Me_2bipy complexes. To assess the space near the axial coordination site (trans to the axial CO), we measured some nonbonded distances from N3 (Supporting Information). For $[Re(CO)_3(L)(HNC(CH_3)N(CH_2CH_2)_2Y)]BF_4$ (Y = CH_2 or NH), the nonbonded distances from N3 to C1 and C10 average ∼0.15 Å longer in 6,6′-Me_2bipy than in 5,5′-Me_2bipy complexes. Properties (such as N−Re−N bond angles) affected by the interior structure have values (Tables 3 and 4) consistent with this additional space. On the other hand, for these same complexes the nonbonded distances from N3 to C4 and C7 average ∼0.5 Å shorter in 6,6′-Me_2bipy than in 5,5′-Me_2bipy complexes. Other properties, such as some NMR shifts, are affected more by the exterior or peripheral structure (see below).

Furthermore, for some properties, the net effects of the differences in the bidentate ligand orientations may cancel. Indeed, regardless of whether the complex has L = 6,6′-Me_2bipy or 5,5′-Me_2bipy, the isomer distribution seems to be unaffected. Thus, for all the complexes in the present study, the repulsions are large enough to favor the presence of only one isomer, namely the *E* isomer.

Our ranking of the expected effects of steric interactions on isomer stability for $[Re(CO)_3(Me_2bipy)(HNC(CH_3)OCH_3)]^+$, $[Re(CO)_3(L)HNC(CH_3)NHR)]^+$, and $[Re(CO)_3(L)(HNC$-

dx.doi.org/10.1021/ic300625n | *Inorg. Chem.* 2012, 51, 7271−7283

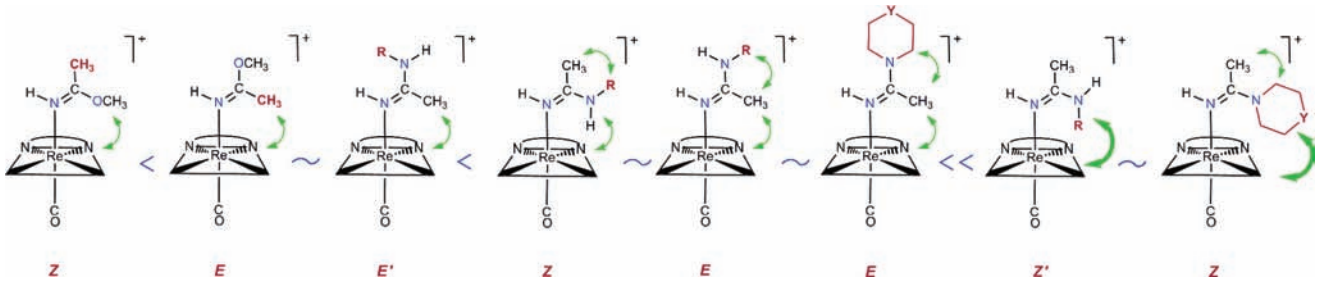

Figure 6. Ranking of increasingly unfavorable total steric repulsive interactions (each double-headed arrow indicates an interaction) in $[Re(CO)_3(Me_2bipy)(HNC(CH_3)OCH_3)]^+$, $[Re(CO)_3(L)HNC(CH_3)NHR)]^+$, and $[Re(CO)_3(L)(HNC(CH_3)N(CH_2CH_2)_2Y)]^+$ complexes [N–N denotes the 5,5′- or 6,6′-Me_2bipy ligands, and Y = CH_2, $(CH_2)_2$, $(CH_2)_3$, NH, or O].

$(CH_3)N(CH_2CH_2)_2Y)]^+$ complexes is shown in Figure 6. This ranking summarizes our experimental observations of the relative isomer abundance of these complexes in this and previous studies.[23,25] This ranking takes into account steric repulsions of the substituents on C_{am} or C_{ie} in the axial with the equatorial Me_2bipy and CO ligands and also the relative repulsions within the amidine ligand between the CH_3 and the NH or NR groups in $[Re(CO)_3(L)HNC(CH_3)NHR)]^+$ complexes. As indicated for the two structures sketched on the far right of Figure 6, the repulsive interactions of the NR substituent with the equatorial ligands depicted in the respective *Z*′ and *Z* sketches are expected to be the most severe. Thus, these interactions are shown with thicker double-headed arrows. The order of the *Z* and *E* isomers of $[Re(CO)_3(L)HNC(CH_3)NHR)]^+$ complexes (fourth and fifth structures from left in Figure 6) reflects our suggestion that the N4H interaction with the equatorial ligands is less repulsive than the corresponding $C_{am}CH_3$ interaction with the equatorial ligands.

Repulsion between the CH_3 and NR groups is secondary and noticeably influences abundance mainly when the two isomers have the same interaction with the equatorial ligands, such as is the case with the *E*′ and *E* isomers of $[Re(CO)_3(L)HNC(CH_3)NHR)]^+$ complexes (third and fifth structures from left in Figure 6). For $[Re(CO)_3(L)HNC(CH_3)NHR)]^+$ complexes,[25] clashes between the NR and the CH_3 amidine substituents destabilize the *E* isomer, which normally has low abundance. The abundance of the *E*′ isomer increased as the steric bulk of the R substituent on C_{am} increased. In turn, the *Z* isomer of $[Re(CO)_3(5,5'\text{-}Me_2bipy)(HNC(CH_3)NH_2)]BF_4$ with similarly sized substituents (NH_2 and CH_3) on C_{am} was highly favored (~ 90% abundant). We caution that the differences in electronic effects influencing the stability of the *Z* and *E* configurations are not known. Nevertheless, the ranking as illustrated in Figure 6 does provide a good guide for predicting the relative abundance of the isomers, especially in polar solvents.

NMR Spectroscopy. All complexes were characterized by ^1H NMR spectroscopy in acetonitrile-d_3; selected complexes were also studied in $CDCl_3$ and DMSO-d_6. ^1H NMR spectra were recorded within at least 6 min of dissolution. In contrast to the spectral data of the previously studied $[Re(CO)_3(5,5'\text{-}Me_2bipy)(HNC(CH_3)NHR)]BF_4$ complexes, all of the ^1H NMR spectra of the new $[Re(CO)_3(L)(HNC(CH_3)N(CH_2CH_2)_2Y)]BF_4$ amidine complexes regardless of the solvent used consistently indicate the presence of only one isomer in solution. Moreover, the spectra of all of these complexes (**3**–**12**) showed no changes with time, even after several days.

The atom numbering system used in this NMR discussion is that shown in Figures 3 and 4. ^1H NMR signals of the bidentate ligand and of N3H were assigned by using the splitting pattern and integration, and by comparison to unambiguous assignments of spectra for previously reported analogous Re^I amidines and iminoether complexes.[23,25]

We illustrate our findings by detailing our studies of compound **3**, $[Re(CO)_3(5,5'\text{-}Me_2bipy)(HNC(CH_3)N(CH_2CH_2)_2CH_2)]BF_4$. When crystals of **3** were dissolved in three different solvents (acetonitrile-d_3, $CDCl_3$, and DMSO-d_6), ^1H NMR spectra showed no evidence for more than one isomer: All peaks in all three solvents remained constant when solutions were monitored from 3 min after dissolution until two weeks. As indicated in our analysis of the C16–N3 bond lengths above, we believe that if the *Z* isomer were present, the interconversion rate would be slow and we would have detected signals for the *Z* isomer. Thus, we are absolutely confident that the *Z* isomer is unstable.

The N3H signal in the new complexes is easily assigned because the peak is a broad singlet integrating to one proton and because it disappeared gradually after the addition of D_2O. For **3**, this N3H signal has a more downfield shift in DMSO-d_6 (5.77 ppm) than in acetonitrile-d_3 (4.78 ppm) or $CDCl_3$ (4.60 ppm). The related values for **4** were 5.32, 4.52, and 4.32 ppm, respectively. A similar NMR dependence of the N3H shift on the solvent was observed for $[Re(CO)_3(5,5'\text{-}Me_2bipy)(HNC(CH_3)OCH_3)]BF_4$; in a standard chloride titration experiment, the downfield shift in DMSO-d_6 was demonstrated to be caused by hydrogen bonding of N3H to DMSO-d_6.[23] In this iminoether complex, as for complexes **3** and **4**, N3H projects out toward the solvent, making this proton available for hydrogen bonding to DMSO-d_6. Such hydrogen bonding explains the solvent dependence found for **3** and **4**.

Dependence on Y of the N3H NMR Signals of $[Re(CO)_3(L)(HNC(CH_3)N(CH_2CH_2)_2Y)]BF_4$, for L = 5,5′-$Me_2$bipy and 6,6′-$Me_2$bipy. Selected ^1H NMR signals of the new amidine complexes (**3**–**12**) in acetonitrile-d_3 are compared in Table 5. For complexes with the amidines having six-membered $N(CH_2CH_2)_2Y$ rings, $[Re(CO)_3(5,5'\text{-}Me_2bipy)(HNC(CH_3)N(CH_2CH_2)_2Y)]BF_4$ (**3**, **6**, and **7**) and $[Re(CO)_3(6,6'\text{-}Me_2bipy)(HNC(CH_3)N(CH_2CH_2)_2Y)]BF_4$ (**8**, **11**, and **12**), the most downfield shift observed for the N3H signal is for the morpholine derivative (Y = O) in each series (4.94 ppm for **7** and 5.30 ppm for **12**). The N3H signal is slightly upfield for piperazine derivatives (Y = NH; 4.84 ppm for **6** and 5.18 ppm for **11**) and farther upfield for piperidine derivatives (Y = CH_2; 4.78 ppm for **3** and 5.14 ppm for **8**). These data indicate that the remote O and N atoms of the morpholine and piperazine derivatives, respectively, exert electron-withdrawing effects on the amidine group, with the more electronegative O atom of the morpholine derivative having the greater downfield-shifting effect on the N3H signal. In the two series, the N3H signal

dx.doi.org/10.1021/ic300625n | *Inorg. Chem.* 2012, 51, 7271–7283

Table 5. ^{1}H NMR Shifts (ppm) for L, N3H, and $C_{am}CH_3$ in $[Re(CO)_3(L)(HNC(CH_3)N(CH_2CH_2)_2Y)]BF_4$ Complexes (Acetonitrile-d_3, 25 °C)

Y	H3/3′	H4/4′	H5/5′	H6/6′	L-CH_3	N3H	$C_{am}CH_3$
			L = 5,5′-Me_2bipy				
CH_2 (**3**)	8.26	8.04		8.85	2.48	4.78	2.10
$(CH_2)_2$ (**4**)	8.27	8.05		8.87	2.48	4.52	2.10
$(CH_2)_3$ (**5**)	8.27	8.04		8.87	2.48	4.49	2.12
NH (**6**)	8.26	8.04		8.85	2.47	4.84	2.12
O (**7**)	8.26	8.04		8.85	2.48	4.94	2.14
			L = 6,6′-Me_2bipy				
CH_2 (**8**)	8.19	8.06	7.62		3.06	5.14	1.60
$(CH_2)_2$ (**9**)	8.19	8.06	7.61		3.07	4.90	1.62
$(CH_2)_3$ (**10**)	8.19	8.07	7.63		3.07	4.82	1.66
NH (**11**)	8.19	8.07	7.62		3.05	5.18	1.63
O (**12**)	8.19	8.07	7.62		3.05	5.30	1.66

systematically shifted upfield as the size of the ring increased from six to seven to eight members. The most upfield N3H shift observed was for the heptamethyleneimine derivatives (Y = $(CH_2)_3$) with the eight-membered ring. The variations in NH shift as the ring size changes can be attributed to a combination of ring-strain, inductive, and solvation effects.

Dependence on L of the $C_{am}CH_3$ NMR Signals of $[Re(CO)_3(L)(HNC(CH_3)N(CH_2CH_2)_2Y)]BF_4$, for L = 5,5′-$Me_2$bipy and 6,6′-$Me_2$bipy. We can readily explain the differences in ^{1}H NMR shifts of the $C_{am}CH_3$ signal between the two series, $[Re(CO)_3(5,5'\text{-}Me_2bipy)(HNC(CH_3)N(CH_2CH_2)_2Y)]BF_4$ (~2.1 ppm, **3**–**7**) and $[Re(CO)_3(6,6'\text{-}Me_2bipy)(HNC(CH_3)N(CH_2CH_2)_2Y)]BF_4$ (~1.6 ppm, **8**–**12**). The shifts are very similar within each of the two series (Table 5). The more upfield shift (by ~0.5 ppm) of the $C_{am}CH_3$ signal for the 6,6′-Me_2bipy complexes (**8**–**12**) than for the 5,5′-Me_2bipy complexes (**3**–**7**) is clearly attributable to the anisotropic effect of the 6,6′-Me_2bipy aromatic ring system. Compared to the $[Re(CO)_3(5,5'\text{-}Me_2bipy)(HNC(CH_3)N(CH_2CH_2)_2Y)]BF_4$ complexes (**3**–**7**), all of the $Re(CO)_3(6,6'\text{-}Me_2bipy)(HNC(CH_3)N(CH_2CH_2)_2Y)]BF_4$ complexes (**8**–**12**) have a shorter distance from the methyl carbon of the amidine ligand (C17) to the centroid of the closest bipyridine ring. This shorter distance results from the tilting in the 6,6′-Me_2bipy ligand, moving the back side of the ring up toward the amidine as discussed above. For example, these distances in $[Re(CO)_3(5,5'\text{-}Me_2bipy)(HNC(CH_3)NC_5H_{10})]BF_4$ (**3**) and $[Re(CO)_3(6,6'\text{-}Me_2bipy)(HNC(CH_3)NC_5H_{10})]BF_4$ (**8**) are 4.2 Å and 3.4 Å, respectively. Therefore, the anisotropic upfield-shifting effect of the bipyridine rings is greater on the $C_{am}CH_3$ methyl signal of $[Re(CO)_3(6,6'\text{-}Me_2bipy)(HNC(CH_3)N(CH_2CH_2)_2Y)]BF_4$ complexes **8**–**12** than on the $C_{am}CH_3$ ^{1}H NMR signal for $[Re(CO)_3(5,5'\text{-}Me_2bipy)(HNC(CH_3)N(CH_2CH_2)_2Y)]BF_4$ complexes **3**–**7**.

The N3H shifts of $[Re(CO)_3(L)(HNC(CH_3)N(CH_2CH_2)_2Y)]BF_4$ complexes for L = 6,6′-Me_2bipy are downfield from the corresponding shifts of the L = 5,5′-Me_2bipy analogues (Table 5). At this time, we cannot identify the reasons for this difference because, as mentioned above, N3H shifts are influenced by a multiplicity of possible factors. In addition, as L is changed, any changes in the heavy-atom anisotropic or inductive effects of the Re will affect the shift.

Dependence of Reaction Times on the Me_2bipy Ligand and the Amine. For a given amine, reactions were relatively faster with $[Re(CO)_3(6,6'\text{-}Me_2bipy)(CH_3CN)]BF_4$ (**2**) than with $[Re(CO)_3(5,5'\text{-}Me_2bipy)(CH_3CN)]BF_4$ (**1**) (Table 6). For

Table 6. Times for Complete Reaction of $[Re(CO)_3(L)(CH_3CN)]BF_4$ Complexes with Heterocyclic Amines ($HN(CH_2CH_2)_2Y$) to Form $[Re(CO)_3(L)(HNC(CH_3)N(CH_2CH_2)_2Y)]BF_4$ Complexes[a]

$HN(CH_2CH_2)_2Y$ (Y)	pK_a	L = 6,6′-Me_2bipy	L = 5,5′-Me_2bipy
piperidine (CH_2)	11.1	≤3 min	<5 min
homopiperidine ($(CH_2)_2$)	10.9	~4.5 min	~8 min
heptamethyleneimine ($(CH_2)_3$)	10.8	~6 min	6 h
piperazine (NH)	10.2	≤3 min	20 min
morpholine (O)	8.5	30 min	4 h

[a]Reaction monitored by NMR spectroscopy in acetonitrile-d_3 at 25 °C.

1 and **2**, the time required for complete reaction, assessed by checking for reaction completion from time to time by NMR spectroscopy (Figure 7), varied with basicity and the ring size of

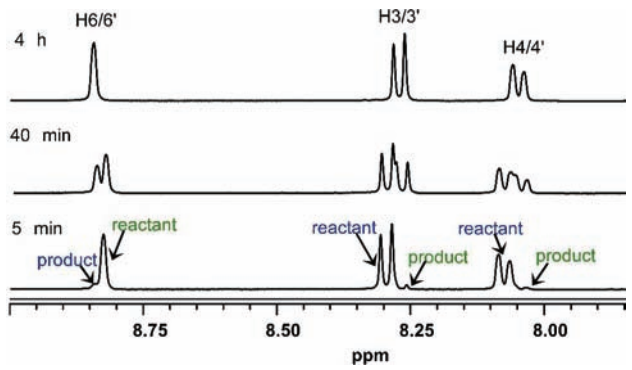

Figure 7. Aromatic region of the ^{1}H NMR spectra in acetonitrile at 25 °C of the reaction of $[Re(CO)_3(5,5'\text{-}Me_2bipy)(CH_3CN)]BF_4$ (**1**) with morpholine to form $[Re(CO)_3(5,5'\text{-}Me_2bipy)(HNC(CH_3)N(CH_2CH_2)_2O)]BF_4$ (**7**).

the heterocyclic amine. The pK_a values of the heterocyclic amines[42] (Table 6) decrease in the order piperidine (with the highest pK_a, 11.1) > homopiperidine > heptamethyleneimine > piperazine > morpholine.[42] The reactions of $[Re(CO)_3(6,6'\text{-}Me_2bipy)(CH_3CN)]BF_4$ (**2**) with piperidine and piperazine were essentially complete before the first spectrum could be recorded (≤3 min). Morpholine, the other six-membered-ring amine, required a much longer reaction time (30 min) owing to its lower basicity (pK_a = 8.5). The same pattern as found for **2** was observed with these heterocyclic amines for **1**. For example, morpholine had the longest reaction completion time (4 h) for the six-membered ring amines with **1** (Figure 7). These results indicate that greater heterocyclic amine basicity is associated with faster reactions, as would be expected. Piperazine has the second lowest pK_a (10.2) compared to the other heterocyclic amines used here; however, the reactions of piperazine with **1** and **2** were relatively fast (≤3 and 20 min, respectively). This relative reactivity can be attributed to the statistical reaction probability for each piperazine molecule (with two amine groups) being twice that of other amines used.

A comparison of reaction completion times for amines with no other heteroatoms in the ring (Table 6) is instructive. For both the $[Re(CO)_3(5,5'\text{-}Me_2bipy)(HNC(CH_3)N(CH_2CH_2)_2Y)]BF_4$ and the $[Re(CO)_3(6,6'\text{-}Me_2bipy)(HNC(CH_3)N$-

dx.doi.org/10.1021/ic300625n | Inorg. Chem. 2012, 51, 7271–7283

$(CH_2CH_2)_2Y)]BF_4$ series, the reaction times increase in the order piperidine < homopiperidine < heptamethyleneimine (Table 6). This finding of longer reaction completion times as the number of amine methylene groups increases makes it clear that steric effects decrease amine reactivity. However, the effect of amine bulk on reaction time is highly pronounced only for heptamethyleneimine with the 5,5′-Me_2bipy complex **1**. The effect is much less pronounced for the 6,6′-Me_2bipy complex **2** because of the greater interior space near the axial coordination site caused by the tilting of the 6,6′-Me_2bipy ligand (as described above).

Reactions of most cyclic secondary amines with $[Re(CO)_3(5,5'\text{-}Me_2bipy)(CH_3CN)]BF_4$ (**1**) reached completion in less than 1 h (Table 6). In contrast, more time was required for reactions of **1** with primary aliphatic amines, even though most of these previously studied amines have a basicity lying within the pK_a range in Table 6. For example, the reaction of $[Re(CO)_3(5,5'\text{-}Me_2bipy)(CH_3CN)]BF_4$ (**1**) required ∼6 h for methylamine (pK_a[43] = 10.6) and ∼4 days for *tert*-butylamine (pK_a[43] = 10.5).[25] Reaction times of $[Re(CO)_3(5,5'\text{-}Me_2bipy)(CH_3CN)]BF_4$ (**1**) and $[Re(CO)_3(6,6'\text{-}Me_2bipy)(CH_3CN)]BF_4$ (**2**) with isopropylamine (pK_a[43] = 10.6) are 28 and 14 h, respectively.[24] These results are consistent with the expected lower nucleophilicity of primary amines as compared with that of the cyclic secondary amines studied here.

Robustness of the Piperidinylamidine Ligation. A 5-fold excess of the relatively basic, strongly coordinating 4-dimethylaminopyridine ligand was added to $[Re(CO)_3(5,5'\text{-}Me_2bipy)(HNC(CH_3)N(CH_2CH_2)_2CH_2)]BF_4$ (**3**) in acetonitrile-d_3 or in $CDCl_3$. No changes in spectral features of **3** were observed for up to two months, indicating that the piperidinylamidine ligand is not readily replaced. The NMR signals for $[Re(CO)_3(5,5'\text{-}Me_2bipy)(4\text{-}dimethylaminopyridine)]BF_4$,[25] synthesized as a control, did not change with time in either acetonitrile-d_3 or $CDCl_3$.

CONCLUSIONS

Unlike previously studied analogous amidine complexes derived from primary amines, all 10 of the $[Re(CO)_3(5,5'\text{- or }6,6'\text{-}Me_2bipy)(HNC(CH_3)N(CH_2CH_2)_2Y)]BF_4$ complexes formed from cyclic secondary amines studied here exist as only one isomer (the *E* isomer) in both the solid state and in solution. These findings are attributable to the combination of the high steric bulk and the C_2 symmetry of the amidine substituents. After dissolution and sufficient time for equilibrium to be established in solution, only the initial *E* isomer was detectable. Thus, the equilibrium between the *Z* and *E* isomers must lie far to the side of the *E* isomer. We conclude that steric repulsions between the $N(CH_2CH_2)_2Y$ groups of the axial amidine ligands and the equatorial ligands preclude formation of any isomer other than *E* (Figures 2 and 6). Nevertheless, these repulsive interactions do not lead to a weakened Re−N3 bond, as indicated by the length of this bond.

The 6,6′-methyl groups in $[Re(CO)_3(6,6'\text{-}Me_2bipy)(HNC(CH_3)N(CH_2CH_2)_2Y)]BF_4$ complexes (**8**−**12**) cause the 6,6′-Me_2bipy ligand to distort and tilt. Although the "front side" of the 6,6′-Me_2bipy ligand with the 6,6′-methyl groups projects down toward the axial CO group, the "back side" of the 6,6′-Me_2bipy ligand projects up. Thus, the 6,6′-Me_2bipy ligand has a net steric footprint comparable to that of the untilted 5,5′-Me_2bipy ligand.

The $[Re(CO)_3(5,5'\text{-}Me_2bipy)(HNC(CH_3)N(CH_2CH_2)_2CH_2)]BF_4$ complex (**3**) in acetonitrile-d_3 or in $CDCl_3$ was robust when challenged with 4-dimethylaminopyridine, indicating that amidine ligands are strong donors. The heterocyclic amines employed here have a relatively high reactivity and form amidines with the *E* configuration only, indicating that amidine complexes can be formed quickly and are isomerically pure. All of these favorable properties cited here suggest that the strategy of using heterocyclic amines to create amidine links to the *fac*-$[M(CO)_3]^+$ core (M = ^{99m}Tc and $^{186/188}$Re radionuclides) may be a useful conjugation method for the development of targeted radiopharmaceuticals.

ASSOCIATED CONTENT

Supporting Information

Crystallographic data for complexes **3**−**12** in CIF format; a figure depicting the overlay of the Re, O1, O2, and O3 atoms in $[Re(CO)_3(5,5'\text{-}Me_2bipy)(HNC(CH_3)N(CH_2CH_2)_2O)]BF_4$ (**7**) and $[Re(CO)_3(6,6'\text{-}Me_2bipy)(HNC(CH_3)N(CH_2CH_2)_2O)]BF_4$ (**12**); a table of selected nonbonded distances for complexes **3**, **6**, **8** and **11**; and a figure depicting the amidine ligand orientation in complexes **4** and **5**. This material is available free of charge via the Internet at http://pubs.acs.org.

AUTHOR INFORMATION

Corresponding Author

*E-mail: lmarzil@lsu.edu.

Notes

The authors declare no competing financial interest.

ACKNOWLEDGMENTS

Purchase of the diffractometer was made possible through grant no. LEQSF(1999-2000)-ENH-TR-13, administered by the Louisiana Board of Regents. This work was supported by the National Institute of Health/National Institute of Diabetes and Digestive and Kidney Diseases (Grant No. R37 DK38842). We thank Gregory T. McCandless for the X-ray crystallographic determination of the structure of complex **3** and for his careful reading of the manuscript.

REFERENCES

(1) Alberto, R. *Eur. J. Nucl. Med. Mol. Imaging* **2003**, *30*, 1299−1302.
(2) Schibli, R.; Schubiger, P. A. *Eur. J. Nucl. Med.* **2002**, *29*, 1529−1542.
(3) Banerjee, S. R.; Maresca, K. P.; Francesconi, L.; Valliant, J.; Babich, J. W.; Zubieta, J. *Nucl. Med. Biol.* **2005**, *32*, 1−20.
(4) Lipowska, M.; Marzilli, L. G.; Taylor, A. T. *J. Nucl. Med.* **2009**, *50*, 454−460.
(5) Bartholomä, M.; Valliant, J.; Maresca, K. P.; Babich, J.; Zubieta, J. *Chem. Commun. (Cambridge, U.K.)* **2009**, 493−512.
(6) Alberto, R. In *Technetium-99m radiopharmaceuticals: status and trends*; International Atomic Energy Agency: Vienna, 2009; pp 19−40.
(7) Wei, L.; Babich, J. W.; Ouellette, W.; Zubieta, J. *Inorg. Chem.* **2006**, *45*, 3057−3066.
(8) Lipowska, M.; He, H.; Malveaux, E.; Xu, X.; Marzilli, L. G.; Taylor, A. T. *J. Nucl. Med.* **2006**, *47*, 1032−1040.
(9) Taylor, A. T.; Lipowska, M.; Marzilli, L. G. *J. Nucl. Med.* **2010**, *51*, 391−396.
(10) Desbouis, D.; Struthers, H.; Spiwok, V.; Küster, T.; Schibli, R. *J. Med. Chem.* **2008**, *51*, 6689−6698.
(11) Abram, U.; Alberto, R. *J. Braz. Chem. Soc.* **2006**, *17*, 1486−1500.
(12) Alberto, R.; Schibli, R.; Abram, U.; Egli, A.; Knapp, F. F.; Schubiger, P. A. *Radiochim. Acta* **1997**, *79*, 99−103.
(13) Alberto, R.; Schibli, R.; Schubiger, A. P.; Abram, U.; Pietzsch, H. J.; Johannsen, B. *J. Am. Chem. Soc.* **1999**, *121*, 6076−6077.

(14) Murray, A.; Simms, M. S.; Scholfield, D. P.; Vincent, R. M.; Denton, G.; Bishop, M. C.; Price, M. R.; Perkins, A. C. *J. Nucl. Med.* **2001**, *42*, 726−732.
(15) Schibli, R.; Schwarzbach, R.; Alberto, R.; Ortner, K.; Schmalle, H.; Dumas, C.; Egli, A.; Schubiger, P. A. *Bioconjugate Chem.* **2002**, *13*, 750−756.
(16) Agorastos, N.; Borsig, L.; Renard, A.; Antoni, P.; Viola, G.; Springler, B.; Kurz, P.; Alberto, R. *Chem.—Eur. J.* **2007**, *13*, 3842−3852.
(17) Cyr, J. E.; Pearson, D. A.; Wilson, D. M.; Nelson, C. A.; Guaraldi, M.; Azure, M. T.; Lister-James, J.; Dinkelborg, L. M.; Dean, R. T. *J. Med. Chem.* **2007**, *50*, 1354−1364.
(18) He, H. Y.; Lipowska, M.; Christoforou, A. M.; Marzilli, L. G.; Taylor, A. T. *Nucl. Med. Biol.* **2007**, *34*, 709−716.
(19) He, H.; Lipowska, M.; Xu, X.; Taylor, A. T.; Marzilli, L. G. *Inorg. Chem.* **2007**, *46*, 3385−3394.
(20) Lipowska, M.; He, H.; Xu, X.; Taylor, A. T.; Marzilli, P. A.; Marzilli, L. G. *Inorg. Chem.* **2010**, *49*, 3141−3151.
(21) Alberto, R. *Eur. J. Inorg. Chem.* **2009**, 21−31.
(22) He, H.; Lipowska, M.; Xu, X.; Taylor, A. T.; Carlone, M.; Marzilli, L. G. *Inorg. Chem.* **2005**, *44*, 5437−5446.
(23) Perera, T.; Abhayawardhana, P.; Fronczek, F. R.; Marzilli, P. A.; Marzilli, L. G. *Eur. J. Inorg. Chem.* **2012**, 616−627.
(24) Perera, T.; Abhayawardhana, P.; Marzilli, P. A.; Fronczek, F. R.; Marzilli, L. G. Manuscript in preparation.
(25) Perera, T.; Fronczek, F. R.; Marzilli, P. A.; Marzilli, L. G. *Inorg. Chem.* **2010**, *49*, 7035−7045.
(26) Wald, J.; Alberto, R.; Ortner, K.; Candreia, L. *Angew. Chem., Int. Ed.* **2001**, *40*, 3062−3066.
(27) Saidi, M.; Seifert, S.; Kretzschmar, M.; Bergmann, R.; Pietzsch, H. J. *J. Organomet. Chem.* **2004**, *689*, 4739−4744.
(28) John, C. S.; Lim, B. B.; Geyer, B. C.; Vilner, B. J.; Bowen, W. D. *Bioconjugate Chem.* **1997**, *8*, 304−309.
(29) Palma, E.; Correia, J. D. G.; Domingos, A.; Santos, I.; Alberto, R.; Spies, H. *J. Organomet. Chem.* **2004**, *689*, 4811−4819.
(30) Seridi, A.; Wolff, M.; Boulay, A.; Saffon, N.; Coulais, Y.; Picard, C.; Machura, B.; Benoist, E. *Inorg. Chem. Commun.* **2011**, *14*, 238−242.
(31) Eicher, T.; Hauptmann, S. *The Chemistry of Heterocycles*, 2nd ed.; WILEY-VCH GmbH & Co. KGaA: Weinheim, Germany, 2003.
(32) Sun, H.; Scott, D. O. *ACS Med. Chem. Lett.* **2011**, *2*, 638−643.
(33) Schmidt, S. P.; Trogler, W. C.; Basolo, F. *Inorg. Synth.* **1990**, *28*, 160−165.
(34) Edwards, D. A.; Marshalsea, J. *J. Organomet. Chem.* **1977**, *131*, 73−91.
(35) Otwinowski, Z.; Minor, W. *Macromolecular Crystallography, Part A, Methods in Enzymology*; New York Academic Press: New York, 1997; Vol. *276*, pp 307−326.
(36) Sheldrick, G. M. *Acta Crystallogr., Sect. A* **2008**, *A64*, 112−122.
(37) Bao, X.; Holt, E. M. *Acta Crystallogr., Sect. C: Cryst. Struct. Commun.* **1992**, *48*, 1655−1657.
(38) Lefèvre, X.; Durieux, G.; Lesturgez, S.; Zargarian, D. *J. Mol. Catal. A: Chem.* **2011**, *335*, 1−7.
(39) Rozenel, S. S.; Kerr, J. B.; Arnold, J. *Dalton Trans.* **2011**, *40*, 10397−10405.
(40) Cini, R.; Caputo, P.; Intini, F. P.; Natile, G. *Inorg. Chem.* **1995**, *182*, 1130−1137.
(41) Liddle, B. J.; Lindeman, S. V.; Reger, D. L.; Gardinier, J. R. *Inorg. Chem.* **2007**, *46*, 8484.
(42) Frenna, V.; Vivona, N.; Consiglio, G.; Spinelli, D. *J. Chem. Soc., Perkin Trans. 2* **1985**, 1865−1868.
(43) Hall, H. K. *J. Am. Chem. Soc.* **1957**, *79*, 5441−5444.